Doppler Spectrum and Second Order Fading Statistics of Emerging 3-D Radio Cellular Propagation Channels

[§]Abrar Ahmed, [§]Sardar Muhammad Gulfam, [§]Syed Junaid Nawaz, and [‡]Mohmammad N. Patwary.

[§]Department of Electrical Engineering, COMSATS Institute of Information Technology, Islamabad, Pakistan.

[‡]Faculty of Computing Engineering and Sciences, Staffordshire University, Stoke-on-trent, UK.

abrar_ahmed@comsats.edu.pk, *sardar_muhammad@comsats.edu.pk*, *junaidnawaz@ieee.org*, and *m.n.patwary@staffs.ac.uk*

Abstract

In implementing fifth generation (5G) networks, the advancements in density of networks, cell size, scale of antenna arrays, communicating nodes mobility, and range of frequencies necessitate to derive a reliable and appropriate channel model. A geometric three dimensional (3-D) tunable channel model is proposed with high degree of flexibility in modelling the orientation, shape, and scale of the scattering region and comprehending the mobility of user terminal. Characterization of second order fading statistics and Doppler spectrum of the radio propagation channel is presented. Mathematical expressions for probability density function (PDF) of Doppler shift and multipath power are derived. The impact of various physical (geometric) channel parameters on statistical characteristics of Doppler spectrum and second order fading statistics is thoroughly analyzed.

Keywords: Doppler Spectrum, Geometric Model, Ellipsoid, Second Order Fading statistics.

I. Introduction

In recent times, work on standardization of fifth generation (5G) has gained the attention of the researchers around the world. Few key things that are to be part of the 5G are millimeter wave (mmWave) spectrum [1], small sized cells [2], less elevated base stations (BS), ultra-densification of the network, massive multiple-input multiple-output (MIMO) [3], and mobility of both ends of the communication link (Device to Device) [4, 5]. The mobility of the communicating nodes imposes Doppler shift, which further leads to time variability in the received signal. With the increase in frequency, the effect of Doppler shift gets more pronounced [6]. So considering the high data rates, high mobility, increased number of users, and higher frequencies of the transmitted signal, it is important to study the second order fading statistics of radio propagation channels.

Many multipath channel models have been proposed in literature in which Doppler shift characteristics have been taken into account. Iltis *et al.* proposed a design for multipath channel communication systems in [7]. Characteristics of spread spectrum system design for underwater and UHF/VHF scenario have been discussed. Expressions for the Doppler spectrum have been derived in [8] for mobile to mobile (M2M) communication scenario. Multipath three dimensional (3-D) scattering environment has been considered and dipole antennas are communicating with mobile units installed in urban areas. It has been claimed that with the accurate knowledge of multipath distribution, real time Doppler spectra can be calculated with different antenna patterns used. A 3-D fading channel model is proposed in [9] and a number of expressions have been derived, which give a direct relationship between power spectral density and

elevation angle of arrival (AoA) of the signal received. A geometrical model is presented in [10] in which single bounce of the multipath components from uniformly distributed scattering objects is assumed. Time of arrival (ToA), AoA, and power of multipath components has been characterized. In [11], tapped delay line channel models have been designed for macro and microcellular environments at 5.3 Ghz. Doppler spectra is seen the be changing with different taps of the designed channel models. Doppler shift distribution of the received signal at MS has been analyzed in [12]. AoA and Doppler shift relation has been utilized to form a relation between PDFs of the Doppler spread and elevation angle. Impact of directional antennas on the Doppler spectra has been discussed in [13]. Relations between PDFs of power, Doppler shift and path distance have been derived in closed form. Also equations for marginal and joint PDFs of power, Doppler shift and elevation AoA have been derived.

Motion of the receiver in a communication system causes rapid fluctuations in the power of the received signal. This effect occurs due to constructive and destructive contribution of the multipath signals reaching at the receiver. Second order fading statistics of the radio channel (like, average fade duration (AFD) and level crossing rate (LCR)) are usually used to study the fading statistics of the channel. The definitions and descriptions of these fading statistics qre given in detail by [14]. Second order fading statistics have been analyzed in [15]. LCR, and AFD have been derived and applied to angular distribution of multipath power of Nakagami-m channel. Various geometric and statistical channel models have been compared on the basis of fading statistics in [16–18]. Effect of changing the Doppler spectrum on the second order fading statistics of these channels has also been analyzed. Recently, an advanced tunable channel model for emerging communication networks is proposed in [19]. The model is tunable with high degrees of flexibility in shaping the scattering region; therefore, it delivers a good fit of analytical results on a diverse range of empirical data sets. The model however only provides analytical expression for plain AoA/ToA characteristics of the channel. Whereas, in studying time variability of the channel characteristics imposed by mobility of the communicating nodes, there is a potential scope to extend the model in [19] from plain AoA/ToA to Doppler spectrum and fading statistics.

This paper extends the tunable 3-D hollow channel model in [19, 20] for quantification of Doppler spectrum, and second order fading statistics. Joint and marginal analytical expressions for multipath power and Doppler shift are derived. Impact of various physical parameters of the channel on fading characteristics is also presented. Rest of the paper is organized as follows: the proposed analytical model for fading channels is explained in sec. II. Derivation of joint and marginal PDFs of the Doppler power spectrum and fading statistics are given in sec. III. Results and discussions are given in section IV. Finally the conclusion in presented in sec. V.

II. System Model

In this section, the proposed 3-D ellipsoidal model is presented. Doppler spectrum and fading statistics of the proposed 3-D model are analyzed. MS is assumed moving with velocity v_m at an instantaneous distance d from BS. The BS is assumed to be fixed at height h_b. The effective scattering region (ESR) is modelled encompassed within the outer bounding semi-ellipsoidal shape and inner bounding hollow elliptical cylindrical shape. Outer bounding ellipsoidal shape is assumed to be scalable along its minor, intermediate, and major axes (a_o, b_o, and c_o) and can be rotated in azimuth plane with an angle θ_o. Inner hollow cylindrical shape is scalable on its major and minor axes with a_i and b_i. The height of inner cylinder is fixed such that it is always greater than c_o so that it hollows the outer bounding ellipsoidal volume vertically. Also the cylinder can be rotated with an angle of θ_i on the azimuth plane. The ESR is designed tunable so that it can adapt any street or road orientation to provide the best results. Direct distance of a certain scattering point (s_p) from the BS and MS is shown by r_b and r_m, respectively. β_m is the elevation angle and ϕ_m is the azimuth angle made by s_p with MS. ϕ_v is the azimuth angle made by the direction of motion of MS and ϕ_r is the azimuth angle between direction of motion of the MS and s_p. ϕ_b and β_b are the azimuth and elevation angles respectively, between BS and s_p. h_e is the height

of cylinder for a given ϕ_m. Scatterers are assumed to be uniformly distributed within the ESR and each scatterer is assumed to scatter a signal in all the directions with equal power. Similarly all the scattered signals received at MS are assumed to have equal power and random phases. Single bounce multipath propagation is assumed. An s_p can be represented by r_{sp}, ϕ_{sp}, and β_{sp} in spherical coordinate system or by x_{sp}, y_{sp}, and z_{sp} in Cartesian coordinate system. The distances of s_p from BS and MS are r_b and r_m, respectively. Total distance which the signal has to travel from BS to MS can thus be given as,

$$l = r_b + r_m. \tag{1}$$

Parameter r_b can be simplified in terms of β_m, r_m, and ϕ_m as shown below,

$$r_b = \sqrt{r_m^2 + d^2 + h_b^2 - 2r_m(d\cos\beta_m\cos\phi_m + h_b\sin\beta_m)}. \tag{2}$$

Substituting (2) in (1) and solving for r_m, we get,

$$r_m = \frac{l^2 - d^2 - h_b^2}{2(l - d\cos\beta_m\cos\phi_m - h_b\sin\beta_m)}. \tag{3}$$

Observing from MS for a direction (ϕ_m, β_m), the distance from MS to the farthest and nearest scattering objects is r_o and r_i, respectively. These distances are given by,

$$r_i = \frac{1}{\cos\beta_m}\sqrt{\frac{2(a_i^2 b_i^2)}{a_i^2 + b_i^2 + (b_i^2 - a_i^2)\cos 2(\theta_i - \phi_m)}}, \tag{4}$$

$$r_o = \frac{a_o b_o c_o}{\sqrt{a_o^2 b_o^2 \sin^2\beta_m + c_o^2\cos^2\beta_m(b_o^2\cos^2(\theta_o - \phi_m) + a_o^2\sin^2(\theta_o - \phi_m))}}. \tag{5}$$

When observing from the MS for a given direction (ϕ_m, β_m), longest and shortest paths can be defined as follows,

$$l_{\min}(\phi_m, \beta_m) = r_i + \sqrt{d^2 + (r_i\cos\beta_m)^2 - 2dr_i\cos\beta_m\cos\phi_m + (h_b - r_i\sin\beta_m)^2}, \tag{6}$$

$$l_{\max}(\phi_m, \beta_m) = r_o + \sqrt{d^2 + (r_o\cos\beta_m)^2 - 2dr_o\cos\beta_m\cos\phi_m + (h_b - r_o\sin\beta_m)^2}. \tag{7}$$

$a_o, b_o, c_o, a_i, b_i, \theta_o$, and θ_i are important geometric parameters of the channel model as they determine the size and orientation of the ESR. This high degree of freedom in geometry of ESR introduces flexibility in obtaining more diverse analytical curves for channel characteristics which helps in achieving a good fit of analytical curves on field measurement results.

III. Channel's Fading Statistics

Propagation of a signal through a wireless channel is characterized by fading. In wireless systems, random process which is linked with fading characterized by their PDF. In this section PDF of Doppler shift is derived for the proposed model and second order statistics are discussed. Azimuth angle ϕ_r shown in Fig. 1, is the angle between direction of MS's motion (ϕ_v) and the angle ϕ_m made by signal arriving from a certain s_p. Hence ϕ_r can be expressed as, $\phi_r = \phi_v - \phi_m$. The relationship of multipath components of the received signal with the Doppler shift can be written as,

$$f_d = f_m\cos\phi_r\cos\beta_m. \tag{8}$$

where f_m is the maximum shift and can be expressed as,

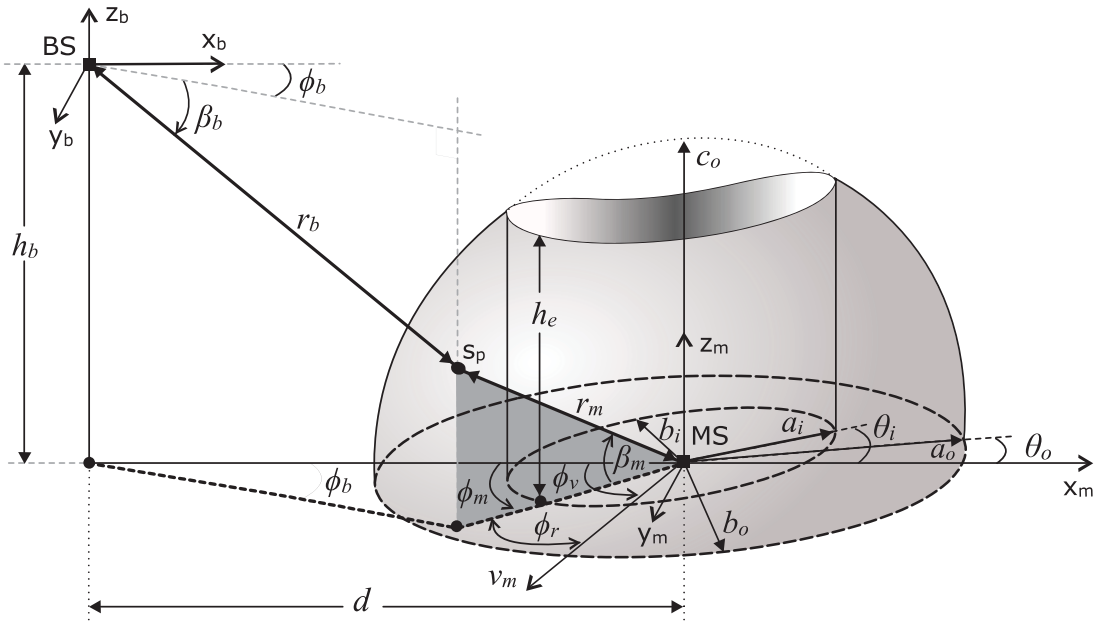

Fig. 1. Proposed Geometric Model for Radio Cellular Communication.

$$f_m = \frac{v}{c} f_c. \tag{9}$$

The normalized Doppler spread $\gamma = f_d/f_m$ can be written as,

$$\gamma = \cos\phi_r \cos\beta_m. \tag{10}$$

The azimuth angle ϕ_m can be expressed as a function of elevation AoA, direction of MS's motion, and Doppler shift as shown below,

$$\phi_m = \phi_v - \cos^{-1}\left(\frac{\gamma}{\cos\beta_m}\right). \tag{11}$$

Equation of joint density function $p(l, \phi_m, \beta_m)$ can be directly used here,

$$p(l, \phi_m, \beta_m) = \frac{p(r_m, \phi_m, \beta_m)}{|J(l, \phi_m, \beta_m)|}. \tag{12}$$

The joint density function for r_m, ϕ_m, and β_m given below is already obtained in [19],

$$p(r_m, \phi_m, \beta_m) = f(x_m, y_m, z_m) r_m^2 \cos\beta_m. \tag{13}$$

$f(x_m, y_m, z_m)$ represents the spatial scatter density function, which is taken as uniform in this model. The Jacobian transformation used in (12) can be derived as,

$$J(l, \phi_m, \beta_m) = \frac{2(d\cos\beta_m\cos\phi_m + h_b\sin\beta_m - l)^2}{l^2 + d^2 + h_b^2 - 2l(d\cos\beta_m\cos\phi_m + h_b\sin\beta_m)}. \tag{14}$$

Substituting the expressions of $p(r_m, \phi_m, \beta_m)$, r_m and $J(l, \phi_m, \beta_m)$ in (12), it can be rewritten as given below,

$$\begin{aligned} p(l, \phi_m, \beta_m) &= f(x_m, y_m, z_m) \\ &\left(\frac{l^2 + d^2 + h_b^2 - 2l(d\cos\beta_m\cos\phi_m + h_b\sin\beta_m)}{8sec\beta_m(d\cos\beta_m\cos\phi_m + h_b\sin\beta_m - l)^4}(l^2 - d^2 - h_b^2)^2\right). \end{aligned} \tag{15}$$

Relationship between power level p_r and length of a multipath propagation path l_p can be written as,

$$p_r = p_o \left(\frac{l_p}{\sqrt{d^2 + h_b^2}} \right)^{-n}. \tag{16}$$

p_o given in (16) is the power of the signal component received from LoS path, n is path loss component, l_p is the propagation length of a specific multipath component from BS to MS, and $\sqrt{d^2 + h_b^2}$ is the line of sight (LoS) propagation path length between BS and MS. Solving for l_p, the above equation can be written as,

$$l_p = \sqrt{d^2 + h_b^2} \left(\frac{p_r}{p_o} \right)^{-\frac{1}{n}}. \tag{17}$$

Joint density function $p(p_r, \phi_m, \beta_m)$ can be derived as,

$$p(p_r, \phi_m, \beta_m) = \left. \frac{p(l_p, \phi_m, \beta_m)}{|J(l_p, \phi_m, \beta_m)|} \right|_{l_p = \sqrt{d^2+h_b^2}\left(\frac{p_r}{p_o}\right)^{-\frac{1}{n}}}. \tag{18}$$

The Jacobean transformation used in (18) is derived as,

$$J(l_p, \phi_m, \beta_m) = \left| \frac{\partial l_p}{\partial p_r} \right|^{-1} = \frac{n p_o}{\sqrt{d^2 + h_b^2}} \left(\frac{p_r}{p_o} \right)^{\frac{n+1}{n}}. \tag{19}$$

Substituting the equation of $J(l_p, \phi_m, \beta_m)$ in (18) the joint density function in terms of 3-D AoA and power level of multipath components can be shown as given below,

$$\begin{aligned} &p(p_r, \phi_m, \beta_m) = \\ &\frac{f(x_m, y_m, z_m) \cos\beta_m \left(d^2 + h_b^2\right)^3 \left(\frac{p_r}{p_o}\right)^{\frac{-3}{n}} \left\{ \left(\frac{p_r}{p_o}\right)^{\frac{2}{n}} - 1 \right\}^2}{8np_r \left(\sqrt{d^2 + h_b^2} - \left(\frac{p_r}{p_o}\right)^{\frac{1}{n}} \left(d\cos\beta_m \cos\phi_m + h_b \sin\beta_m\right) \right)^4} \\ &\times \left[\sqrt{d^2 + h_b^2} \left\{ \left(\frac{p_r}{p_o}\right)^{\frac{2}{n}} + 1 \right\} - 2 \left(\frac{p_r}{p_o}\right)^{\frac{1}{n}} \right. \\ &\left. \left(d\cos\beta_m \cos\phi_m + h_b \sin\beta_m\right) \right]. \end{aligned} \tag{20}$$

Joint density function $p(p_r, \gamma, \beta_m)$ can thus be expressed as,

$$p(p_r, \gamma, \beta_m) = \left. \frac{p(p_r, \phi_m, \beta_m)}{|J(p_r, \phi_m, \beta_m)|} \right|_{\phi_m = \phi_v - \cos^{-1}\left(\frac{\gamma}{\cos\beta_m}\right)}. \tag{21}$$

The Jacobean transformation for p_r, ϕ_m, and β_m can be derived as shown below,

$$J(p_r, \phi_m, \beta_m) = \left| \frac{\partial \phi_m}{\partial \gamma} \right|^{-1} = \sqrt{\cos^2\beta_m - \gamma^2}. \tag{22}$$

Substituting the expression of Jacobean transform from (22) in (21) and letting $\psi = (p_r/p_o)^{-1/n}$, joint density function of power level, Doppler spread, and elevation angle β_m can be expressed as,

$$\begin{aligned} p(p_r, \gamma, \beta_m) = \sum_{i=1}^{2} &\left\{ \left(\frac{(d^2+h_b^2)^3 (\psi^2 - 1) \psi^{n+1} f(x_m, y_m, z_m)}{8np_o \sqrt{1 - \gamma^2 sec^2 \beta_m}} \right) \right. \\ &\left. \times \left(\frac{d^2 + h_b^2(1+\psi^2) - 2\psi(d\cos\beta_m \cos\phi_i + h_b \sin\beta_m)}{(d\cos\beta_m \cos\phi_i + h_b \sin\beta_m - (d^2+h_b^2)\psi)^4} \right) \right\}. \end{aligned} \tag{23}$$

Integrating (23) over β_m and p_r, respectively, gives the marginal PDF of the Doppler spectrum characteristics of the proposed model.

$$p(\gamma) = \int_0^{\frac{\pi}{2}} \int_{p_l}^{p_u} \sum_{i=1}^{2} \left\{ \left(\frac{(d^2+h_b^2)^3(\psi^2-1)\psi^{n+1} f(x_m,y_m,z_m)}{8np_o\sqrt{1-\gamma^2 sec^2\beta_m}} \right) \times \left(\frac{d^2+h_b^2(1+\psi^2)-2\psi(d\cos\beta_m\cos\phi_i+h_b\sin\beta_m)}{(d\cos\beta_m\cos\phi_i+h_b\sin\beta_m-(d^2+h_b^2)\psi)^4} \right) \right\} \mathrm{d}p_r \mathrm{d}\beta_m. \tag{24}$$

p_l and p_u are dependant on the path lengths of the multipath components. The signal received from the longest propagation path has minimum power, while the signal arrived from the shortest propagation path hold the highest power. p_u and p_l, can be shown shown below,

$$p_u = p_o \left(\frac{l_{\min}}{\sqrt{d^2+h_b^2}} \right)^{-n}, \tag{25}$$

$$p_l = p_o \left(\frac{l_{\max}}{\sqrt{d^2+h_b^2}} \right)^{-n}. \tag{26}$$

Integrating (24) over normalized Doppler shift gives the cumulative distribution function (CDF) of the Doppler spectrum as shown below,

$$F_\Gamma(\gamma) = \int_{-1}^{\gamma} p(\Gamma) d\Gamma. \tag{27}$$

CDF of the received signal gives better insight of amount of received gain and the time duration for which it remains below a certain (under observation) threshold level. The complex received signal is $r(t) = \sum_{i=0}^{L-1} \alpha_i e^{j2\pi f_{d_i} t}$, where f_{d_i} represents the Doppler shift experienced by i^{th} multipath component as expressed in (8) and L is the total number of multipath components. High order statistics gives more analytical plateform to analyze the signal. The analysis is extended to study second-order fading statistics, which are joint distribution of the envelope and its derivative with respect to time. These fading statistics includes LCR (N_R), and AFD ($\bar{\tau}$), can be defined as below. LCR of any random process gives useful information about the underlying process, and is widely used in many engineering fields. In channel modeling, LCR is associated with some important characteristics of the channel like handoff, AFD, fading rate, movement of MS, and the effect of diversity on fading. LCR is the count of how many times the signal crosses the threshold level, ($\rho = R/R_{\text{RMS}}$) , i.e., measurement of how rapid the fading occurs and general expression of LCR is given by [14] and shown below,

$$N_R = \int_0^{\infty} \dot{r} p(R, \dot{r}) d\dot{r} \tag{28}$$

AFD ($\bar{\tau}$) is the time duration for which a signal stays below a certain (under observation) threshold level (ρ) and can be defined as below,

$$\bar{\tau} = \frac{1}{N_R} \int_0^{R} p(r) dr \tag{29}$$

IV. Results and Discussions

Analytical results for Doppler shift characteristics of the proposed model are presented in Fig. 2, where the impact of various important physical parameters of the model is presented. Change in behavior of the Doppler spectrum with variation in the ratio between major (a_o) and intermediate (b_o) axes of the outer bounding ellipsoid is shown in Fig. 2(a). It can be seen that as the ESR transforms from spherical to elliptical shape in azimuthal plane, the slope of CDF changes from frequency flat to frequency variant. This employs that PDF of Doppler shift transforms from flat to U shaped form. In Fig. 2(b), the impact of size of inner hollow cylinder for a given ϕ_v is analyzed on the Doppler shift. It is evident from the figure

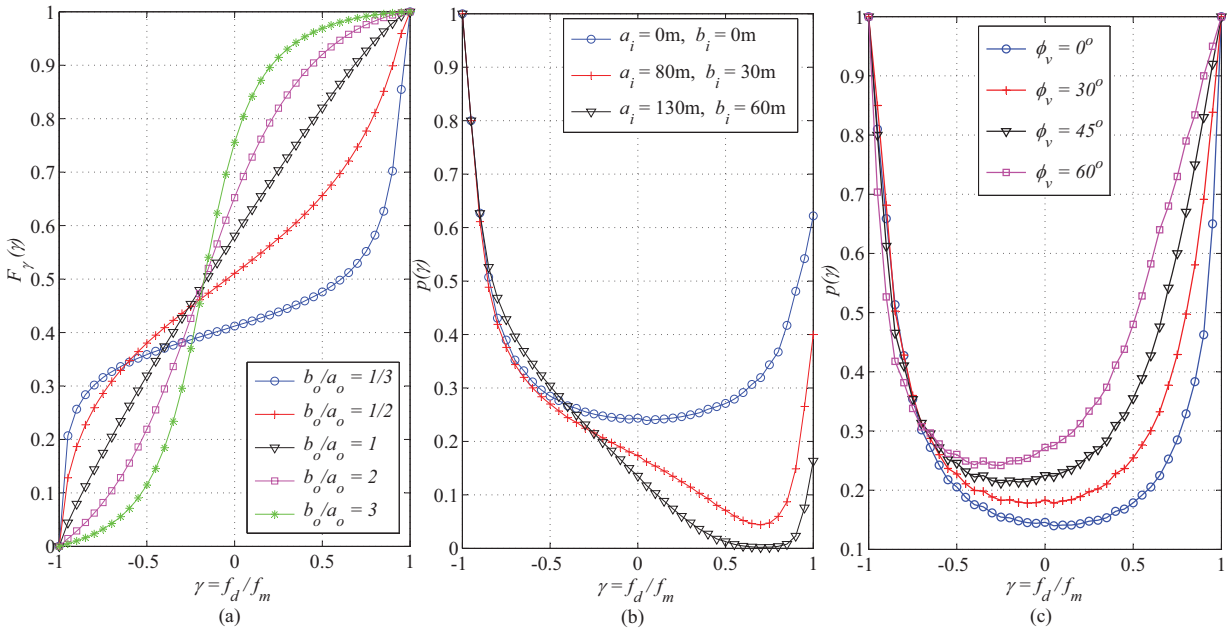

Fig. 2. The impact of variation in (a) the ratio b_o/a_o on the CDF, (b) the size of inner hollow cylinder on PDF, and (c) ϕ_v on PDF of Doppler shift characteristics.

that as the ESR becomes more hollow from inside, the PDF of Doppler shift tends to tilt more on one side (positive in this scenario) of the γ. This is because the scatterers contributing in positive and/or negative Doppler shift increase and/or decrease according to the orientation and scale of the inner bounding hollow elliptical cylinder as compared to outer bounding ellipsoid. The direction of MS's motion (ϕ_v) w.r.t. LoS direction has a significant impact on the Doppler shift characteristics when the geometric composition of ESR is uneven; which is shown in Fig. 2(c) for a specific scenario. It can be seen that when the MS moves directly towards the BS (i.e., $\phi_v = 0^o$), the scattering objects contributing in a shift towards positive and negative side are evenly balanced, therefore the PDF is balanced U-shaped. For higher values of ϕ_v, the PDF skews towards positive or negative side depending upon the shape of the ESR. The impact of variation in the ratio b_o/a_o, size of inner hollow cylinder, and ϕ_v on the LCR is shown in Fig. 3 (a), (b), and (c), respectively. It has been observed in Fig. 3(a) that change in the ratio between major (a_o) and intermediate (b_o) axes of the outer bounding ellipsoid effects LCR linearly. Peak of LCR is observed at $\rho = -1$, and the curves drop sharply for higher values of ρ. It can be seen in Fig. 3(b) that effect of reducing the scatterers in the local vicinity of MS is non linear. The impact of direction of MS's motion ϕ_v on LCR (see Fig. 3(c)) is also observed as non linear. The impact of variation in the ratio b_o/a_o, size of inner hollow cylinder, and ϕ_v on the AFD is shown in Fig. 4 (a), (b), and (c), respectively. It can be seen in Fig. 4(a) that AFD increases linearly with increase in the ratio b_o/a_o because of transformation of the ESR. Fig. 4(b) shows the non linear increment in AFD with increase in the hollowness of the ESR, which means that with less number of scatterers present in the close vicinity of the MS, the fading time of the channel increases. Similar non linear increase in AFD is observed in Fig. 4(c) with change in the direction of motion of MS.

It can be seen from the graphs shown that by changing the geometrical parameters of the model, it is convenient to increase/decrease the second order fading statistics parameters and hence the proposed model can take shape of any orientation of the physical scenario. The proposed geometric channel model provides high degrees of freedom in designing the physical dimensions and orientations of the scattering region's boundaries and therefore can be tuned to realistically model the propagation scenarios for obtaining more realistic angular statistics. The angular spread of multipath waves in a rich multipath environment highly

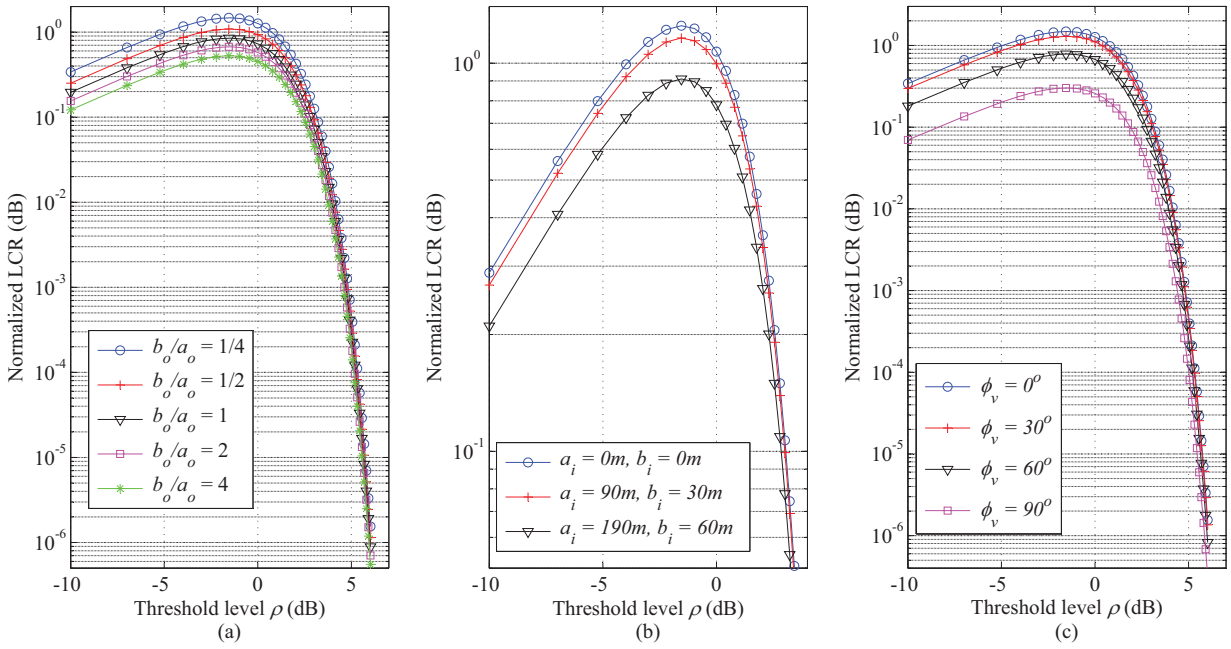

Fig. 3. The impact of variation in the (a) ratio b_o/a_o, (b) size of inner hollow cylinder, and (c) ϕ_v, on the LCR.

influences the Doppler spectrum, which further determines the time variability of channel characteristics. Therefore, the proposed analytical results on Doppler spectrum are of high significance in studying the time varying characteristics of highly dynamic propagation scenarios of emerging cellular communication networks.

V. Conclusion

Second order fading statistics of the emerging land mobile radio propagation channels has been presented in this paper. Joint and marginal mathematical expressions for distribution characteristics of Doppler shift and multipath power have been derived for the advanced tunable 3-D hollow geometric scattering model. Doppler shift characteristics have been analyzed and the impact of various physical channel parameters on its statistical characteristics has been discussed. Finally, the analysis has been further extended for the characterization of second order fading statistics of radio communication channel.

Acknowledgements

The authors would like to acknowledge the travel grant support by HEC Pakistan to attend the conference. A part of this research work was supported by the EU ATOM-690750 research project approved under the call H2020-MSCA-RISE-2015.

References

[1] G. R. MacCartney, J. Zhang, S. Nie, and T. S. Rappaport., "Path loss models for 5G millimeter wave propagation channels in urban microcells," in *Proc. of IEEE Global Commun. Conf., Exhibition and Industry Forum (GLOBECOM13)*, Dec. 2013, pp. 3948 – 3953.

[2] V. Jungnickel, K. Manolakis, W. Zirwas, B. Panzner, V. Braun, M. Lossow, M. Sternad, R. Apelfröjd, and T. Svensson, "The role of small cells, coordinated multipoint, and massive MIMO in 5G," *IEEE Commun. Mag.*, pp. 44–51, May 2014.

[3] E. G. Larsson, O. Edfors, F. Tufvesson, and T. L. Marzetta, "Massive MIMO for next generation wireless systems," *IEEE Commun. Mag.*, pp. 186–195, Feb. 2014.

[4] S. J. Nawaz, M. Riaz, N. M. Khan, and S. Wyne, "Temporal analysis of a 3D ellipsoid channel model for the vehicle-to-vehicle communication environments," *Wireless Pers. Commun.*, vol. 82, no. 3, pp. 1337–1350, 2015.

[5] S. Biswas, R. Tatchikou, and F. Dion, "Vehicle-to-vehicle wireless communication protocols for enhancing highway traffic safety," *IEEE Commun. Mag.*, vol. 44, no. 1, pp. 74–82, 2006.

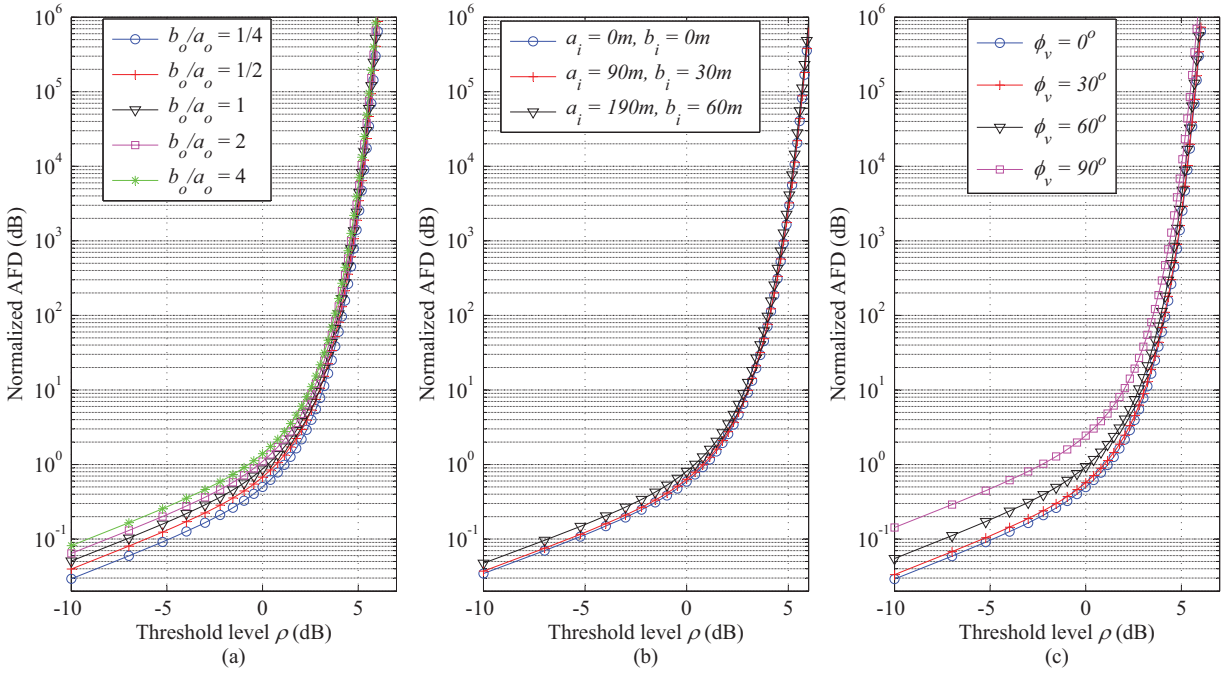

Fig. 4. The impact of variation in the (a) ratio b_o/a_o, (b) size of inner hollow cylinder, and (c) ϕ_v, on the AFD.

[6] J. Andrews, S. Buzzi, W. Choi, S. Hanly, A. Lozano, A. Soong, and J. Zhang, "What will 5G be?" *IEEE J. on Selected Areas in Commun.*, vol. 32, no. 6, pp. 1065–1082, Jun. 2014.

[7] R. Iltis and A. W. Fuxjaeger, "A digital DS spread-spectrum receiver with joint channel and Doppler shift estimation," *IEEE Trans. on Commun.*, vol. 39, no. 8, pp. 1255–1267, 1991.

[8] F. Vatalaro and A. Forcella, "Doppler spectrum in mobile-to-mobile communications in the presence of three-dimensional multipath scattering," *IEEE Trans. on Veh. Technol.*, vol. 46, no. 1, pp. 213–219, 1997.

[9] S. Qu and T. Yeap, "A three-dimensional scattering model for fading channels in land mobile environment," *IEEE Trans. on Veh. Technol.*, vol. 48, no. 3, pp. 765–781, 1999.

[10] P. Petrus, J. H. Reed, and T. S. Rappaport, "Geometrical-based statistical macrocell channel model for mobile environments," *IEEE Trans. on Commun.*, vol. 50, no. 3, pp. 495–502, 2002.

[11] X. Zhao, J. Kivinen, P. Vainikainen, and K. Skog, "Characterization of Doppler spectra for mobile communications at 5.3 GHz," *IEEE Trans. on Veh. Technol.*, vol. 52, no. 1, pp. 14–23, 2003.

[12] S. Qu, "An analysis of probability distribution of Doppler shift in three-dimensional mobile radio environments," *IEEE Trans. on Veh. Technol.*, vol. 58, no. 4, pp. 1634–1639, May 2009.

[13] S. J. Nawaz, N. M. Khan, M. N. Patwary, and M. Moniri, "Effect of directional antenna on the Doppler spectrum in 3-D mobile radio propagation environment," *IEEE Trans. on Veh. Technol.*, vol. 60, no. 7, pp. 2895–2903, Sep. 2011.

[14] G. D. Durgin and T. S. Rappaport, "Theory of multipath shape factors for small-scale fading wireless channels," *IEEE Trans. on Antenna and Propag.*, vol. 48, no. 5, pp. 682–693, May 2000.

[15] J. hua Lu and Y. Han, "Application of multipath shape factors in Nakagami-m fading channel," in *Proc. of Int. Conf. on Wireless Commun. Signal Process.*, Nov. 2009, pp. 1–4.

[16] Z. M. loni and N. M. Khan, "Analysis of fading statistics based on geometrical and statistical channel models," in *Proc. of Int. Conf. on Emerging Technol. (ICET)*, Oct. 2010, pp. 221–225.

[17] Z. M. Loni, R. Ullah, and N. M. Khan, "Analysis of fading statistics based on angle of arrival measurements," in *Proc. of Int. Workshop on Antenna Technol. (IWAT)*, Mar. 2011, pp. 314–319.

[18] Z. M. loni and N. M. Khan, "Analysis of fading statistics in cellular mobile communication systems," *The J. of Supercomputing*, vol. 64, no. 2, pp. 295–309, 2013.

[19] A. Ahmed, S. J. Nawaz, and S. M. Gulfam, "A 3-D propagation model for emerging land mobile radio cellular environments," *PLoS ONE*, vol. 10, no. 8, p. e0132555, 2015.

[20] A. Ahmed, S. J. Nawaz, N. M. Khan, M. N. Patwary, and M. Abdel-Maguid, "Angular characteristics of a unified 3-D scattering model for emerging cellular networks," in *Proc. of IEEE Int. Conf. on Commun. (ICC)*, Jun. 2015, pp. 2450–2456.